The Influence of Rainfall Classification on Bias Correction of Satellite Precipitation Products Power Merra-2, Gsmap, and Persiann-Ccs

Irene Baria[1]*, Anak Agung Ngurah Satria Damarnegara[2], Mohammad Bagus Ansori[3]

[1,2,3] Fakultas Teknik Sipil, Perencanaan, Dan Kebumian, Institut Teknologi Sepuluh Nopember, Indonesia
* Corresponding Author:
Email: irenebaria.ac@gmail.com

Abstract.

This study evaluates the effectiveness of six bias correction methods, namely Linear Scaling, Delta, second- and third-order Polynomial, Quantile Mapping, and Hybrid Polynomial–Quantile Mapping, in improving satellite-based precipitation estimates and assessing the performance of three satellite rainfall products through validation and verification processes. In addition, the influence of rainfall classification on validation results is examined. Model performance is evaluated using the correlation coefficient, percent bias (PBIAS), Nash–Sutcliffe efficiency (NSE), and the ratio of RMSE to standard deviation (RSR). The results indicate that PERSIANN-CCS, despite having the smallest grid size and the highest spatial resolution, exhibits greater rainfall variability and lower agreement with rain gauge observations, particularly during extreme and minimum rainfall events. In contrast, GSMaP and Power MERRA-2 demonstrate rainfall patterns that are more consistent with observed data. Rainfall classification shows that the calibration dataset consists of 60% normal years and 40% wet years, with no dry years, while the verification dataset does not include wet-year conditions. Based on the calibration and validation results, Power MERRA-2 corrected using the third-order polynomial method provides the best performance at daily, monthly, and annual timescales. Verification results indicate satisfactory performance at monthly and annual scales, as well as improved daily-scale performance under normal-year verification scenarios, supported by cumulative distribution function (CDF) analysis

Keywords: *Calibration; Merra-2; Gsmap; Persiann-CCS and Rainfall Classification.*

I. INTRODUCTION

The Manikin Watershed is administratively located within Kupang Regency and Kupang City, East Nusa Tenggara Province (NTT), Indonesia. Based on the outlet coordinates of the Manikin water level gauging station, the watershed is situated at 10°08′29.4″ S and 123°41′22.7″ E [1]. The Manikin Watershed plays a crucial role in supplying water resources to parts of Kupang Regency, particularly for irrigation and other water demands. This importance is indicated by the presence of three operational irrigation weirs and one dam currently under construction in the upstream area [2]. The existence of this infrastructure highlights the necessity for efficient and sustainable water resources management, which inevitably requires accurate and comprehensive hydrological data. However, the availability of rainfall data in the Manikin Watershed remains a significant challenge. At present, four rainfall gauging stations exist within the watershed; nevertheless, during the most recent minimum ten-year period, these stations exhibit data gaps over several time intervals [2]. Such data discontinuities can hinder long-term hydrological analyses. In particular, statistical methods for design flood estimation require at least ten years of continuous and complete rainfall data to produce reliable results [3]. The insufficiency of data from existing rain gauges has made the need for alternative data sources increasingly urgent. As a solution, satellite-based precipitation data have been widely adopted as an alternative source, especially for filling missing or unavailable rainfall records. Several satellite precipitation products commonly used in hydrological studies include Power MERRA-2, GSMaP, and PERSIANN.

These products offer extensive spatial and temporal coverage with consistent data availability, enabling rainfall monitoring in regions with limited ground-based observation networks. The spatial resolutions of these satellite products differ, with Power MERRA-2 providing a resolution of 0.5° × 0.625° [4], GSMaP 0.1° × 0.1° [5], and PERSIANN-CCS 0.04° × 0.04° [6].Nevertheless, satellite precipitation data cannot directly replace ground-based observations without prior validation. Each satellite product employs different estimation algorithms, spatial resolutions, and data assimilation techniques, which may lead to discrepancies relative to actual field conditions. To ensure the reliability of satellite data for water resources analysis, their quality must be evaluated using suitability and agreement parameters against available rain gauge observations. This validation process is essential, as satellite data exhibiting high correlation with

measured rainfall are more likely to yield river discharge estimates with minimal bias and greater representativeness of real hydrological conditions [7]. This assertion is consistent with findings reported in Civilla: Jurnal Teknik Sipil Universitas Islam Lamongan, which emphasize that although satellite rainfall data offer advantages in terms of accessibility and spatial coverage, adjustment to ground observations is still required to ensure the validity and accuracy of hydrological outputs, such as design rainfall maps [8].

Based on a literature review of satellite rainfall analyses conducted in NTT Province, four related studies have been identified, including evaluations of PERSIANN-CDR [9], GPM [10], TRMM [11], and combined analyses of GPM, GSMaP, and CHIRPS [12]. However, to date, no study has comprehensively compared the performance of three satellite precipitation products—Power MERRA-2, GSMaP, and PERSIANN-CCS—against rain gauge data while simultaneously analyzing the influence of rainfall classification (wet, normal, and dry years) on validation results.Therefore, this study aims to apply six bias correction methods—Linear Scaling [13], Delta [14], second- and third-order Polynomial [15], Quantile Mapping [16,17], and Hybrid Polynomial–Quantile Mapping [18]—to satellite precipitation data and to evaluate the performance of the three satellite products through validation and verification analyses. In addition, the study investigates the effect of rainfall classification on validation outcomes. Validation performance is assessed using correlation coefficient interpretation, Percent Bias (PBIAS), Nash–Sutcliffe Efficiency (NSE), and the Ratio of Root Mean Square Error to the Standard Deviation of Observations (RSR) [19]. The results of this study are expected to provide recommendations on the most representative satellite precipitation product and its corresponding bias correction equations for the Manikin Watershed, as well as to serve as a reference for bias correction analysis of highly variable rainfall data in hydrological studies conducted in regions with limited observational data.

II. METHODS

This study adopts a quantitative research design with an evaluative and comparative approach, aiming to evaluate and compare the performance of satellite-based precipitation products—Power MERRA-2, GSMaP, and PERSIANN-CCS—against observed rainfall data in the Manikin Watershed. The study begins with the collection of rainfall observations from rain gauge stations influencing the Manikin Watershed, obtained from the Nusa Tenggara II River Basin Authority (BBWS Nusa Tenggara II) [1] and the Meteorology, Climatology, and Geophysics Agency (BMKG) of Kupang [23], followed by data correction procedures.Topographic data collection includes the identification of the watershed outlet point and the acquisition of the National Digital Elevation Model (DEM) [24]. Topographic analysis is conducted by delineating the watershed and sub-watershed boundaries using the National DEM and outlet coordinates in HEC-HMS software, with the resulting watershed boundary serving as a reference for satellite data extraction.Satellite precipitation data are downloaded in hourly format for the period from 31 December 2003 to 31 December 2020, corresponding to the overlapping data availability of the three satellite products and rain gauge observations within the Manikin Watershed.

For GSMaP and PERSIANN-CCS, spatial data in NetCDF (.nc) format are extracted and converted into comma-separated values (.csv) format using QGIS software to enable further processing in spreadsheet applications. After sorting the data according to the temporal format, temporal alignment between satellite data recorded in Coordinated Universal Time (UTC) and rain gauge observation times is performed [25]. In this study, a 15-hour time offset is applied, accounting for the 8-hour difference between Central Indonesia Time (WITA) and UTC, in addition to the rain gauge observation time at 07:00 local time [27].Subsequently, the data are aggregated into daily, monthly, and annual periods using Pivot Table and Power Query tools for data filtering and processing in Microsoft Excel. Areal rainfall analysis is then conducted according to the spatial coverage of each data source, resulting in a single representative rainfall time series for each dataset, which enables subsequent comparison and validation prior to bias correction.Calibration, validation, and verification analyses are performed using RStudio (R version 4.5.1) with the R programming language. Data calibration is carried out using six bias correction methods over the calibration period of 2004–2013, resulting in correction equations for each satellite product and each temporal aggregation period.

Following bias correction, validation metrics are recalculated for the corrected satellite data, allowing assessment of correction performance based on differences between validation results before and after correction.The derived correction equations are subsequently applied to satellite precipitation data for the verification period of 2014–2020. Verification scenarios are developed using the same six bias correction methods and are further analyzed based on rainfall year classification (wet, normal, and dry). The final analysis involves validation of the verification results to identify the optimal combination of satellite product and bias correction method based on validation performance.To facilitate interpretation, validation results for uncorrected satellite data, bias-corrected data from the calibration process, and verification outcomes are summarized for each temporal aggregation period and correction method. Additionally, bias correction performance is illustrated using scatter plots, cumulative distribution function (CDF) plots, and time series analyses, which serve as the basis for drawing conclusions and formulating recommendations from this study.

Description and Technical

The data received at the Data Processing Center were first sorted according to their temporal sequence to form time series datasets. These time series were then subjected to consistency testing using the Double Mass Curve (DMC) method [20] and the Rescaled Adjusted Partial Sums (RAPS) method [21]. After the data were corrected and confirmed to be consistent, the analysis proceeded with the calculation of areal average rainfall using the Thiessen polygon method [22].Calibration was performed using six bias correction methods, namely Linear Scaling [13], Delta [14], second- and third-order Polynomial Regression [15], Quantile Mapping [16,17], and Hybrid Polynomial–Quantile Mapping [18], as described below.

1) Linear Scaling $P_{corr} = P_{sat} \times \frac{\overline{P_{obs}}}{\overline{P_{sat}}}$ This method is implemented in RStudio using the mean() function and vector operations.	Notation: Pcorr = bias-corrected precipitation Psat = satellite precipitation $\overline{P_{obs}}$ = mean observed precipitation $\overline{P_{sat}}$ = mean satellite precipitation
2) Delta $P_{corr} = P_{sat} \times \frac{\overline{P_{obs}}}{\overline{P_{sat}}}$	Mathematically, this formulation is identical to the Linear Scaling method; however, its application context differs, particularly in climate change impact studies. In RStudio, this method is implemented using mean statistics and vector multiplication operations.
3) Polynomial Regression Orde 2 $P_{obs} = aP_{sat}^2 + bP_{sat} + c$ RStudio implementation: lm(P obs ~ poly(P sat, 2, raw = TRUE))	Pobs = observed precipitation Psat = satellite precipitation a, b, dan c = regression coefficients estimated using the least squares method
4) Polynomial Regression Orde 3 $P_{obs} = aP_{sat}^3 + bP_{sat}^2 + cP_{sat} + d$ RStudio implementation: lm(P obs ~ poly(P sat, 3, raw = TRUE))	Pobs = observed precipitation Psat = satellite precipitation a, b, c, d = regression coefficients estimated using the least squares method
5*) Quantile Mapping* $P_o = F_o^{-1}(F_m(P_m))$ This method is implemented in RStudio using the qmap package, specifically the functions fitQmapQUANT() and doQmapQUANT().	P_m = precipitation value from the model/satellite product F_m = umulative distribution function (CDF) of the model data $F_m(P_m)$ = quantile (cumulative probability) of Pm based on the model distribution F_o^{-1} = inverse cumulative distribution function (inverse CDF) of observed precipitation P_o = bias-corrected precipitation consistent with the observed distribution
6) Hybrid Polynomial–Quantile Mapping Stage 1: Polynomial Regression: $P' = f(P_{sat})$ Stage 2: Quantile Mapping (QM) $P_{corr} = F_{obs}^{-1}(F_{P'}(P'))$ In RStudio, this method is implemented by combining the lm() function with the qmap package.	P ′ = preliminary bias-corrected precipitation (mm) Psat = satellite precipitation f(·) = polynomial regression function representing the nonlinear relationship between satellite and observed precipitation Pcorr = inal bias-corrected precipitation FP′(·) = cumulative distribution function (CDF) of polynomial-corrected precipitation Fobs−1(·) = inverse cumulative distribution function (inverse CDF) of observed precipitation

To evaluate the performance of the bias correction results, model performance tests were conducted using statistical parameters as suggested by Moriasi et al. [19] [30], who classified statistical validation metrics into several categories:

Table 1. Satellite Data Validation Assessment Criteria

Performance Rating	RSR	NSE	PBIAS	Performance Rating	Correlation Value
Very Good	0.00 ≤ RSR ≤ 0.50	0.75 < NSE ≤ 1.00	PBIAS < ± 10%	Very Low	0 – 0,19
Good	0.50 < RSR ≤ 0.60	0.65 < NSE ≤ 0.75	± 10 ≤ PBIAS < ± 15%	Low	0,20 – 0,39
Satisfactory	0.60 < RSR ≤ 0.70	0.50 < NSE ≤ 0. 65	± 15 ≤ PBIAS < ± 25%	Moderate	0,40 – 0,59
Unsatisfactory	RSR > 0.70	NSE ≤ 0.50	PBIAS ≥ ± 25%	Strong	0,60 – 0,79
				Very Strong	0,81 - 1

Source: Moriasi et al. (2007) Mukaka (2012).

III. RESULT AND DISCUSSION

Rain Post Data Analysis

Rain gauge data analysis involves compiling rainfall station records to determine total precipitation over specific periods, along with the geographic coordinates of each station. The analysis includes double mass curve testing to assess data consistency and areal rainfall estimation using the Thiessen polygon method. This study analyzes data from four rainfall stations within the Manikin Watershed, as presented in **Table 2.** The dataset used was aligned with the availability of both satellite precipitation data and institutional rainfall records. Consequently, the most complete and comparable dataset spans the period from 2004 to 2020.Following data compilation, missing rainfall records were identified at the MRG Tarus and MRG Tilong stations for several months in the years 2009, 2012, and 2019. These data gaps were filled using the Inverse Square Distance (ISD) method [28] to ensure data continuity for subsequent analyses.

Table 2. Rain Post Data

No	Rain Post Name	Coordinate UTM Zone 51S		Data source
		X	Y	
1	Baun	579206.64	8861915.41	BMKG Kupang
2	El Tari-Penfui	572599.35	8874949.6	BMKG Kupang
3	Tarus	574500.73	8879478.51	BWS NT II
4	Tilong	581310.11	8875961.53	BWS NT II

Source:Data Collection Results (2025).

Double Mass Curve Test of Rainfall Post Data

This method is performed by comparing the cumulative rainfall of a selected rain gauge station with the cumulative rainfall of surrounding stations, which is then plotted on a double mass curve graph. Data consistency is assessed based on the deviation of the slope angle from the normal range ($42° \leq \alpha \leq 48°$) [20]. The results of the double mass curve consistency test for the rain gauge data are presented in **Figure** and **Table 3**.

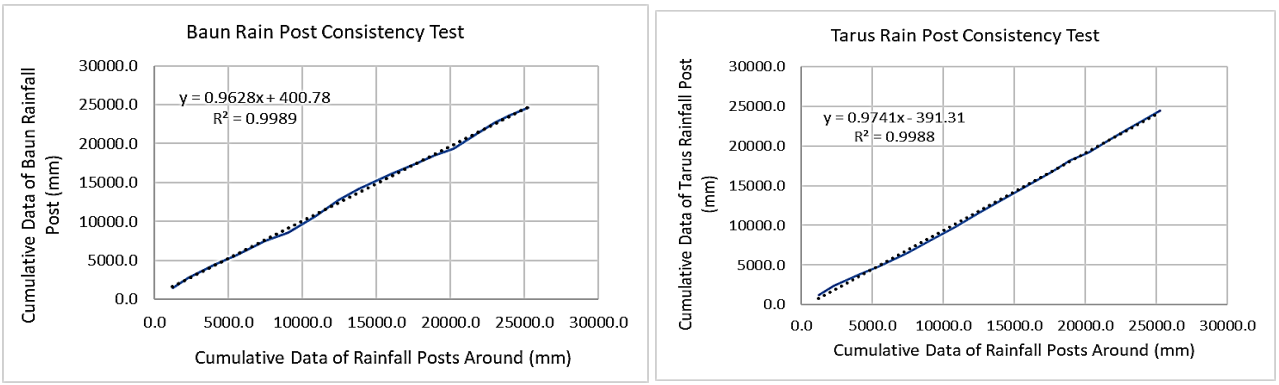

Source: Analysis Results (2025).

Fig 1. Recapitulation of the test curve of the double mass curve of rainfall post data in the Manikin watershed

Table 3. Recapitulation of the Alpha Angle of the Rain Post

No.	Rain Post Name	S	α	Status
1	MRG Baun	0.98	44.31	Consistent
2	MRG El Tari-Penfui	1.01	45.42	Consistent
3	MRG Tarus	0.97	44.15	Consistent
4	MRG Tilong	1.01	45.43	Consistent

Source: Analysis Results (2025).

Average Rainfall Analysis of Rainfall Post Areas

The Thiessen polygon delineation for the Manikin Watershed was performed using QGIS software through the Vector → Geometry Tools → Voronoi Polygons function. The resulting spatial distribution of rainfall station influence areas is presented in **Figure 2.**

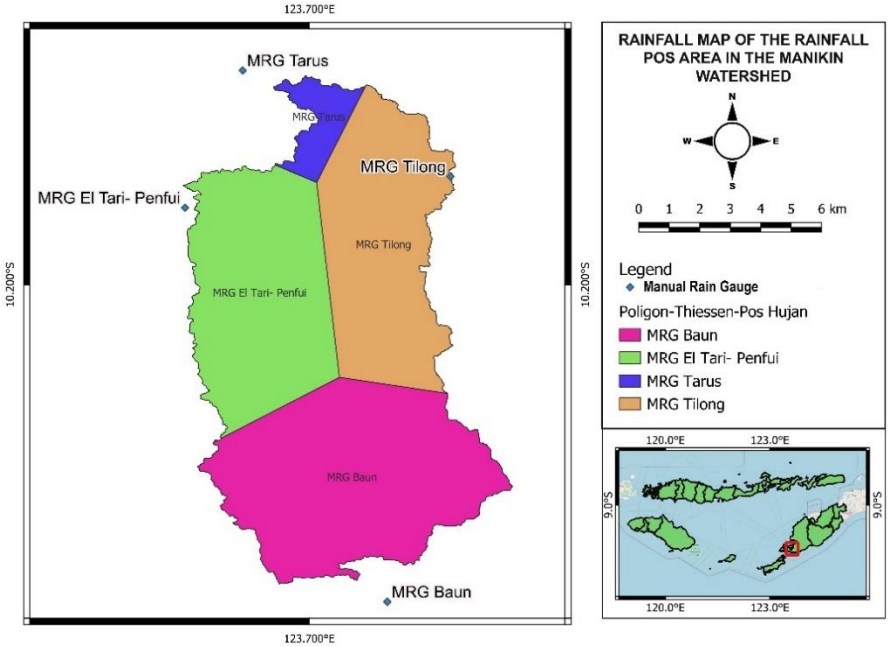

Source: Analysis Results (2025).

Fig 2. Rainfall Map of Rainfall Post Area in Manikin Watershed

After determining the area of each Thiessen polygon corresponding to the respective rain gauge stations, the relative coefficient (Kr) was subsequently calculated for each station.

Table 4. Relative Coefficient Value of Thiessen Polygon Rainfall Post in Manikin Watershed

No.	Rain Post Name	Area (m2)	Kr
1	MRG Baun	44331150.4	0.384
2	MRG El Tari- Penfui	34254669.15	0.296
3	MRG Tarus	4722796.44	0.041
4	MRG Tilong	32258345.1	0.279
	Total	**115566961.1**	**1.000**

Source: Analysis Results (2025).

Analysis of Average Rainfall Area Satellite Rainfall Data

Satellite precipitation data used in this study consist of three products: Power MERRA-2, GSMaP, and PERSIANN-CCS. PERSIANN-CCS provides precipitation grids with a spatial resolution of 0.04° × 0.04°, equivalent to approximately 4.4 × 4.4 km, GSMaP has a grid resolution of 0.1° × 0.1°, equivalent to approximately 11.05 × 11.05 km, and Power MERRA-2 has a grid resolution of 0.5° × 0.625°, equivalent to approximately 55.3 × 69.1 km (based on a conversion factor of 1 degree at the equator equal to 110.567 km). Subsequently, satellite precipitation data were aggregated from hourly to daily, monthly, and annual time scales after temporal adjustment, and the datasets were organized using Microsoft Excel Pivot Table and Power Query tools for data filtering and processing.Prior to converting NetCDF files to CSV format, spatial grids influencing the Manikin Watershed were selected. Power MERRA-2 utilized two grids, GSMaP four grids, and PERSIANN-CCS fourteen grids. Thiessen coefficients were then calculated for the precipitation grids of each satellite product with respect to the Manikin Watershed.

Table 5. Relative Coefficient Values of Thiessen Polygons of MERRA-2 Satellite Power in Manikin Watershed

Grid No. Power MERRA-2	Area (m2)	Kr
1	85977868.81	0.744
2	29589092.28	0.256
Total	**115566961.1**	**1.000**

Source: Analysis Results (2025).

Table 6. Relative Coefficient Values of GSMap Satellite Thiessen Polygons in the Manikin Watershed

Grid No. GSMap	Area (m2)	Kr
1	17055862.15	0.148
2	32007961.83	0.277
3	44811524.63	0.388
4	21691612.48	0.188
Total	**115566961.1**	**1.000**

Source: Analysis Results (2025).

Table 7. Relative Coefficient Values of PERSIAN-CCS Satellite Thiessen Polygons in the Manikin Watershed

Grid No. PERSIAN-CCS	Area (m2)	Kr	Grid No. PERSIAN-CCS	Area (m2)	Kr
1	92327.26	0.0008	8	193240.44	0.0017
2	65687.01	0.0006	9	14497065	0.1254
3	7166079.9	0.062	10	19192608	0.1661
4	16598527.5	0.1436	11	3416709.1	0.0296
5	470216.67	0.0041	12	6437112.9	0.0557
6	17024691.1	0.1473	13	10876188	0.0941
7	17757692.4	0.1537	14	1778816.6	0.0154
			Total	**115566961**	**1**

Source: Analysis Results (2025).

Based on regional rainfall calculations [22] from the Rain Post and 3 satellites studied, which are shown in the following graph.

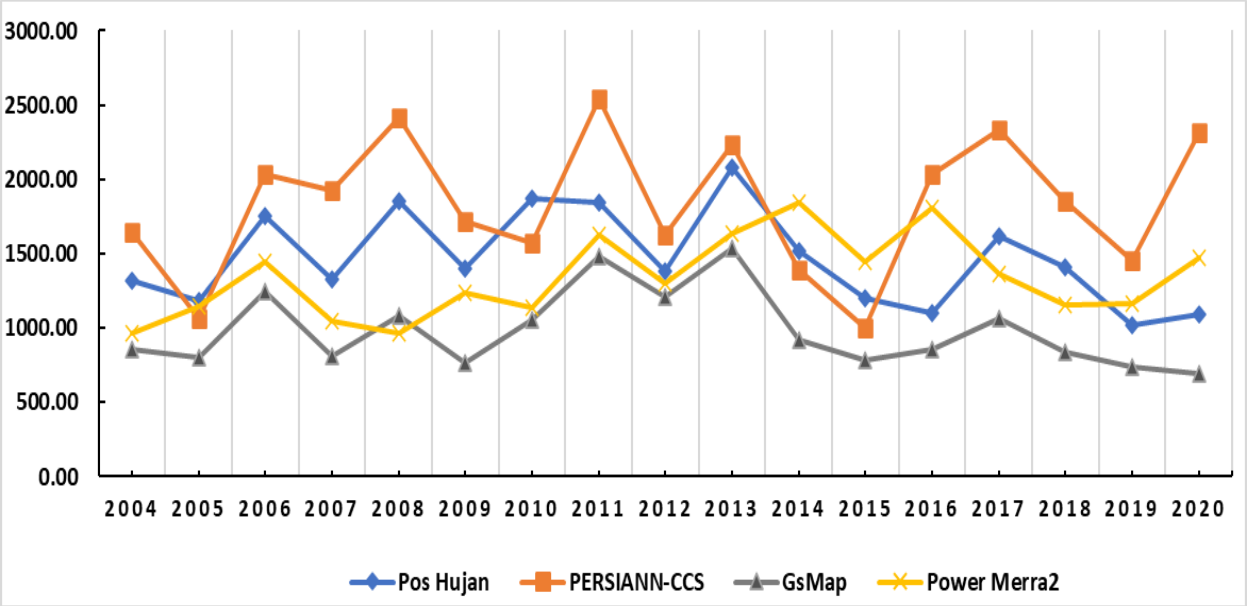

Source: Analysis Results (2025).

Fig 3. Annual Rainfall Recapitulation Graph for the Region, Rainfall Post Data, MERRA-2 Power Satellite, PERSIANN-CCS Satellite and GSMap

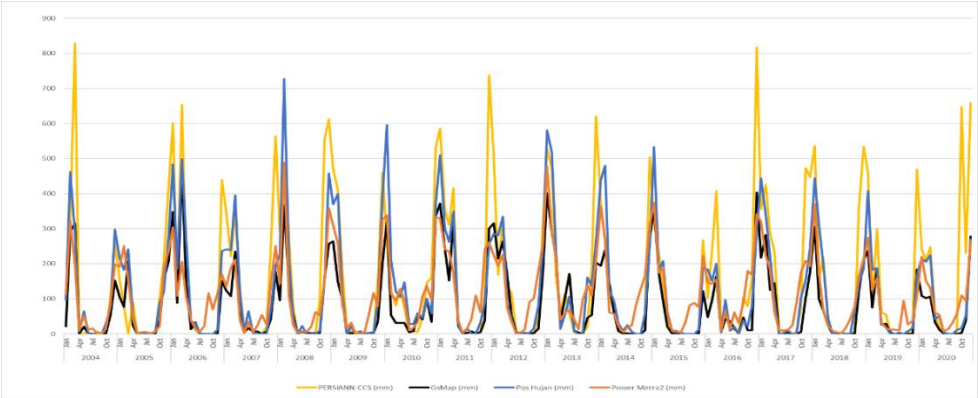

Source: Analysis Results (2025).

Fig 4. Monthly Rainfall Recapitulation Graph for the Region, Rainfall Post Data, MERRA-2 Power Satellite, PERSIANN-CCS Satellite and GSMap

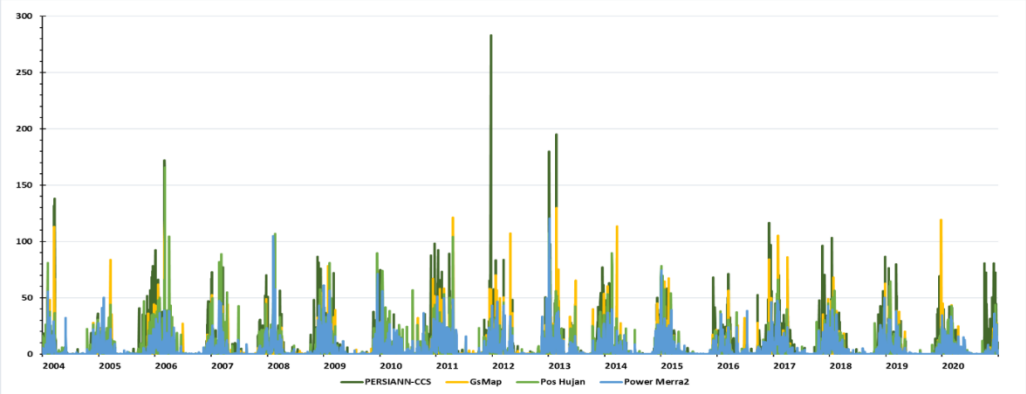

Source: Analysis Results (2025).

Fig 5. Daily Rainfall Recapitulation Graph for the Region, Rainfall Post Data, MERRA-2 Power Satellite, PERSIANN-CCS Satellite and GSMap

Areal Average Rainfall Analysis of Satellite Precipitation Data

According to Soemarto, the hydrological conditions of a region are not constant, as annual rainfall exhibits continuous fluctuations; therefore, it is essential to identify years that represent dry, normal, and wet conditions [29]. Based on this classification, calibration and verification scenarios for data analysis can be developed accordingly.

Year	2004	2005	2006	2007	2008	2009	2010	2011	2012	2013	2014	2015	2016	2017	2018	2019	2020	Legend:
Rainy Year Classification																		Wet
Calibration																		Normal
Verification 1																		Dry
Verification 2																		
Verification 3																		

Source: Analysis Results (2025).

Fig 6. Calculation Scenario Based on Rainy Year Classification

Calibration of Satellite Precipitation Data

The bias correction analysis employed in this study includes Linear Scaling, the Delta Method, second- and third-order polynomial regression, Quantile Mapping, and Hybrid Polynomial–Quantile Mapping. Performance evaluation was conducted using the R software environment, supported by the openxlsx and dplyr packages for data processing, and the Metrics and hydroGOF packages for statistical computations, including RMSE, NSE, RSR, and PBIAS. The fitQmapQUANT and doQmapQUANT functions were utilized for the implementation of the Quantile Mapping method. Result visualization was performed using the ggplot2 package, and all outputs were exported to Excel format using the writexl package.

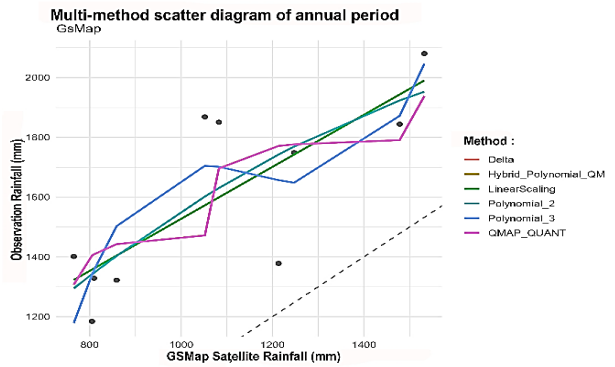

Satellite	Method	Equality
GsMap	Polynomial_3	1748.012237 + -1.23483x + 0.000697x^2
GsMap	Polynomial_2	-786.872079 + 1.995508x + -0.000308x^2
GsMap	LinearScaling	118.709618 + 1.271122x + -0.000203x^2
GsMap	Delta	-968.324727 + 2.334232x + -0.000443x^2
GsMap	Hybrid_Polynomial_QM	1486.730974 + -0.590245x + 4e-04x^2
GsMap	QMAP_QUANT	1490.832305 + -0.594874x + 0.000401x^2
PERSIANN-CCS	Polynomial_3	774.93782 + 0.011035x + 0.00031x^2
PERSIANN-CCS	Polynomial_2	-31.308351 + 1.039941x + -1.3e-05x^2
PERSIANN-CCS	Delta	859.699676 + 0.422845x + 2.3e-05x^2
PERSIANN-CCS	LinearScaling	744.463902 + 0.480758x + 3.2e-05x^2
PERSIANN-CCS	Hybrid_Polynomial_QM	408.311134 + 0.841298x + -5.8e-05x^2
PERSIANN-CCS	QMAP_QUANT	408.087259 + 0.841586x + -5.8e-05x^2
Power_Merra2	Polynomial_3	-189.572195 + 1.24093x + -7.5e-05x^2
Power_Merra2	Polynomial_2	12.205979 + 0.984485x + 5e-06x^2
Power_Merra2	Delta	376.09194 + 0.673623x + 5.5e-05x^2
Power_Merra2	LinearScaling	511.325616 + 0.6096x + 4.2e-05x^2
Power_Merra2	Hybrid_Polynomial_QM	-1046.725192 + 2.563644x + -0.00055x^2
Power_Merra2	QMAP_QUANT	-1046.928412 + 2.563938x + -0.00055x^2

Source: Analysis Results (2025).

Fig 7. Satellite Rain Data Calibration Results Annual Period

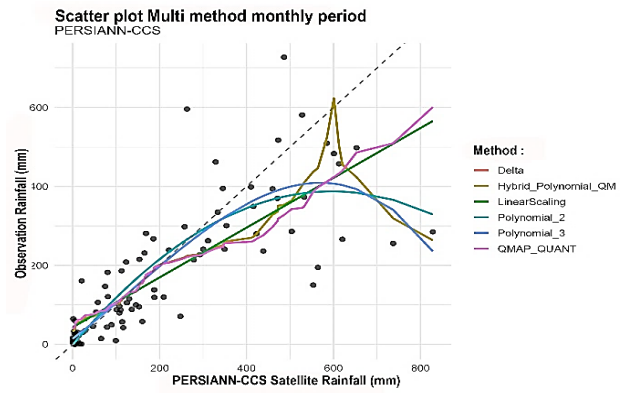

Satellite	Method	Equality
GsMap	Polynomial_3	0.336046 + 0.99449x + 1.2e-05x^2
GsMap	Polynomial_2	0.129756 + 0.997869x + 5e-06x^2
GsMap	LinearScaling	18.320058 + 0.982701x + -0.000247x^2
GsMap	Delta	-66.259711 + 1.518703x + -0.000543x^2
GsMap	Hybrid_Polynomial_QM	3.109472 + 1.123179x + -0.000425x^2
GsMap	QMAP_QUANT	3.107346 + 1.123219x + -0.000425x^2
PERSIANN-CCS	Polynomial_3	0.78281 + 0.984887x + 3.7e-05x^2
PERSIANN-CCS	Polynomial_2	17.088965 + 0.596588x + 0.001063x^2
PERSIANN-CCS	Delta	41.091646 + 1.2299x + -0.001091x^2
PERSIANN-CCS	LinearScaling	-1.493379 + 1.554201x + -0.001552x^2
PERSIANN-CCS	Hybrid_Polynomial_QM	-2.021678 + 1.356686x + -0.001033x^2
PERSIANN-CCS	QMAP_QUANT	-13.308623 + 1.607051x + -0.001586x^2
Power_Merra2	Polynomial_3	0.262548 + 0.996242x + 7e-06x^2
Power_Merra2	Polynomial_2	0.720934 + 0.989612x + 2e-05x^2
Power_Merra2	LinearScaling	3.802038 + 0.806109x + 0.000599x^2
Power_Merra2	Delta	-25.068862 + 0.922638x + 0.000879x^2
Power_Merra2	Hybrid_Polynomial_QM	15.639051 + 0.927335x + -5e-05x^2
Power_Merra2	QMAP_QUANT	15.635619 + 0.927425x + -5.1e-05x^2

Source: Analysis Results (2025).

Fig 8. Satellite Rain Data Calibration Results Monthly Period

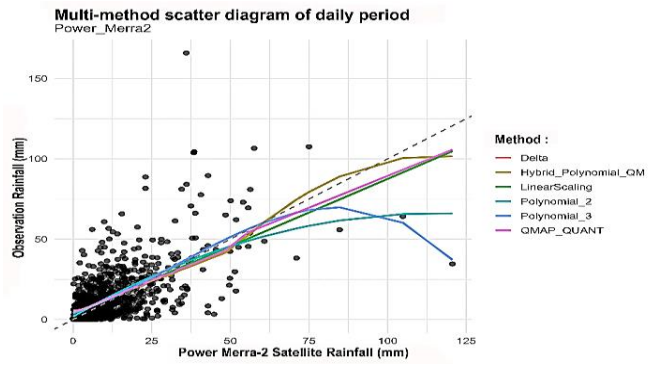

Satellite	Method	Equality
GsMap	Polynomial_3	1.676183 + 0.813716x + 0.003409x^2
GsMap	QMAP_QUANT	7.301042 + 0.449274x + -0.000132x^2
GsMap	Hybrid_Polynomial_QM	7.290367 + 0.450993x + -0.000162x^2
GsMap	Polynomial_2	-0.1717 + 1.019535x + -0.00038x^2
GsMap	LinearScaling	8.781617 + 0.341978x + -8.9e-05x^2
GsMap	Delta	7.259595 + 0.457719x + -0.000159x^2
PERSIANN-CCS	Polynomial_3	2.655102 + 0.690702x + 0.00735x^2
PERSIANN-CCS	Hybrid_Polynomial_QM	9.527611 + 0.287289x + -0.000294x^2
PERSIANN-CCS	Polynomial_2	4.144286 + 0.476124x + 0.014343x^2
PERSIANN-CCS	QMAP_QUANT	9.412944 + 0.301406x + -0.000389x^2
PERSIANN-CCS	LinearScaling	9.670964 + 0.298264x + -0.000697x^2
PERSIANN-CCS	Delta	10.507398 + 0.231647x + -0.000432x^2
Power_Merra2	Polynomial_3	0.193067 + 0.974776x + 0.000507x^2
Power_Merra2	Hybrid_Polynomial_QM	3.622977 + 0.813522x + -0.002705x^2
Power_Merra2	Polynomial_2	1.58402 + 0.771783x + 0.00523x^2
Power_Merra2	QMAP_QUANT	3.582216 + 0.818378x + -0.002724x^2
Power_Merra2	LinearScaling	1.828416 + 0.959456x + -0.003577x^2
Power_Merra2	Delta	-0.264386 + 1.134074x + -0.00484x^2

Source: Analysis Results (2025).

Fig 9. Satellite Rain Data Calibration Results Daily Period

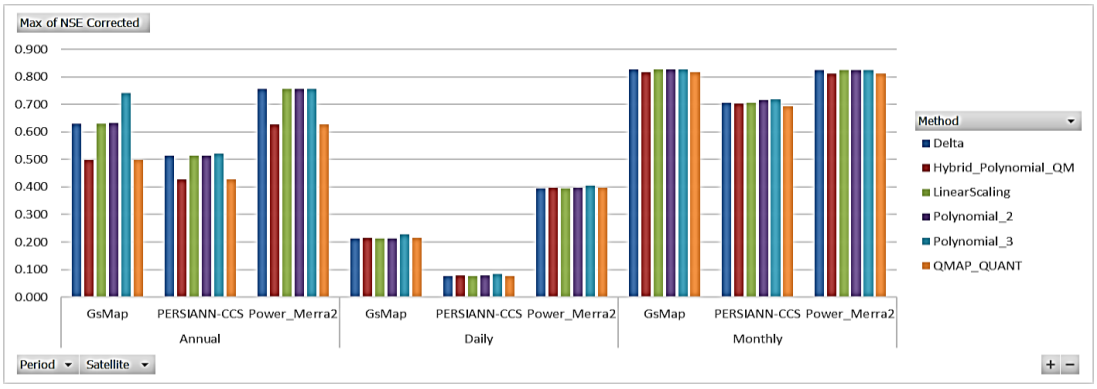

Source: Analysis Results (2025).

Fig 10. Comparison of NSE values based on calibration results

Calibration was performed by applying bias correction and validation for all methods across each temporal period and for all satellite products examined. Based on the calibration results, data interpretation was subsequently conducted using validation performance metrics, as summarized in **Table 1.** Based on the calibration results, the best-performing method was selected according to the validation metrics for each data period—daily, monthly, and annual—and for each satellite product, as presented in the tables below.

Table 8. Comparison of Satellite Data Validation Before and After Daily Period Correction

Period	Satellite	Original RMSE	NSE Original	RSR Original	Original Correlation	PBIAS Original
Daily	Power_Merra2	12.839	0.351	0.805	0.615	14.032
Daily	GsMap	17.185	-0.163	1.078	0.460	25.114
Daily	PERSIANN-CCS	25.094	-1.480	1.574	0.272	-27.058
Method	**Satellite**	**Corrected RMSE**	**NSE Corrected**	**Corrected RSR**	**Corrected Correlation**	**Corrected PBIAS**
Polynomial_3	Power_Merra2	12.290	0.405	0.771	0.637	0.000
Polynomial_3	GsMap	14.014	0.227	0.879	0.476	0.000
Polynomial_3	PERSIANN-CCS	15.262	0.083	0.957	0.288	0.000

Source: Analysis Results (2025).

Table 9. Comparison of Satellite Data Validation Before and After Monthly Period Correction

Period	Satellite	Original RMSE	NSE Original	RSR Original	Original Correlation	PBIAS Original
Monthly	Power_Merra2	0.739	0.508	0.904	17.414	0.739
Monthly	GsMap	0.671	0.570	0.908	32.552	0.671
Monthly	PERSIANN-CCS	0.371	0.789	0.791	-19.252	0.371
Method	**Satellite**	**Corrected RMSE**	**NSE Corrected**	**Corrected RSR**	**Corrected Correlation**	**Corrected PBIAS**
Polynomial_3	Power_Merra2	69.703	0.826	0.415	0.909	0.000
Polynomial_3	GsMap	70.167	0.824	0.418	0.908	0.000
Polynomial_3	PERSIANN-CCS	88.824	0.717	0.529	0.847	0.000

Source: Analysis Results (2025).

Table 10. Comparison of Satellite Data Validation Before and After Annual Period Correction

Period	Satellite	Original RMSE	NSE Original	RSR Original	Original Correlation	PBIAS Original
Annual	Power_Merra2	249.140	0.278	0.806	0.869	249.140
Annual	GsMap	404.785	-0.905	1.309	0.717	404.785
Annual	PERSIANN-CCS	547.980	-2.492	1.773	0.789	547.980
Method	**Satellite**	**Corrected RMSE**	**NSE Corrected**	**Corrected RSR**	**Corrected Correlation**	**Corrected PBIAS**
Polynomial_3	Power_Merra2	144.798	0.756	0.468	0.870	0.000
Polynomial_3	GsMap	149.311	0.741	0.483	0.861	0.000
Polynomial_3	PERSIANN-CCS	203.217	0.520	0.657	0.721	0.000

Source: Analysis Results (2025).

Based on the calibration and validation results, the Power MERRA-2 satellite product corrected using the third-order polynomial method exhibited the best validation performance among the other five methods across the daily, monthly, and annual periods.

Verification of Satellite Precipitation Data

The verification process was conducted by applying the regression equations of the selected method to the selected satellite product under the scenarios illustrated in **Figure 6.** Verification Scenario 1 consists of 50% normal and 50% dry years, Verification Scenario 2 comprises 100% normal years, and Verification Scenario 3 comprises 100% dry years. The results of the verification analysis, presented in terms of validation metrics, cumulative distribution function (CDF) plots, and time series graphs, are shown below.

Table 11. Validation Results of Verification 1

Period	RSR	NSE	Correlation	PBIAS	RSR Criteria	NSE Criteria	RSR CDF	NSE CDF
Daily	0.786	0.382	0.631	-7.954	Unsatisfactory	Unsatisfactory	0.264	0.930
Monthly	0.487	0.759	0.886	-7.399	Very Good	Very Good	0.289	0.916
Annual	0.603	0.575	0.894	-7.927	Satisfactory	Satisfactory	0.615	0.619

Source: Analysis Results (2025).

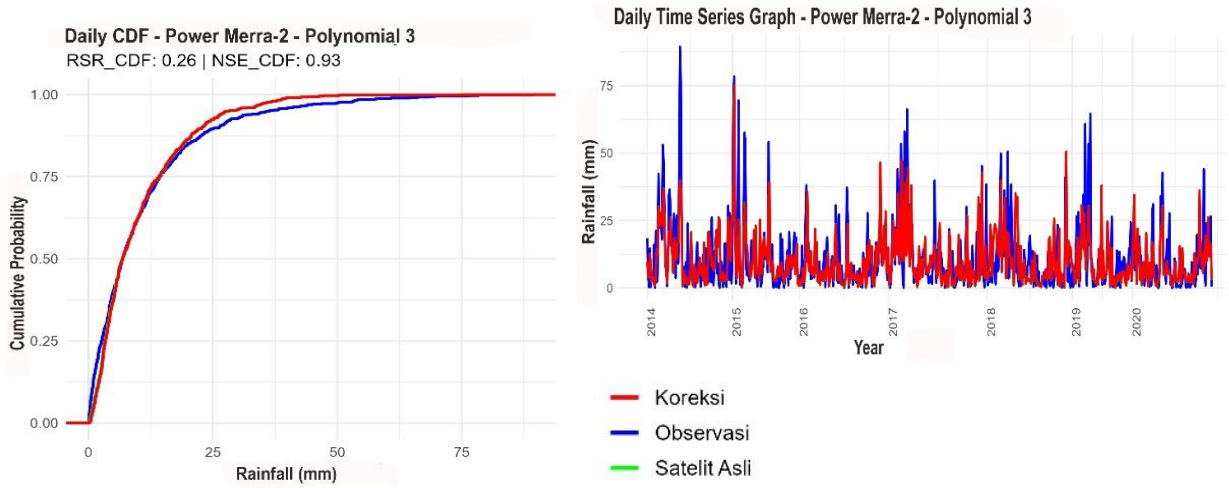

Source: Analysis Results (2025).

Fig 11. CDF Graph and Time Series Results of Verification 1

Table 12. Validation Results of Verification 2

Period	RSR	NSE	Correlation	PBIAS	RSR Criteria	NSE Criteria	Criteria Correlation	PBIAS Criteria
Daily	0.677	0.539	0.744	-9.773	Satisfactory	Satisfactory	Strong	Very Good
Monthly	0.486	0.747	0.931	-19.671	Very Good	Good	Very Strong	Satisfactory
Annual	0.512	0.475	1.000	-7.764	Good	Unsatisfactory	Very Strong	Very Good

Source: Analysis Results (2025).

Table 13. Validation Results of Verification 3

Period	RSR	NSE	Correlation	PBIAS	RSR Criteria	NSE Criteria	Criteria Correlation	PBIAS Criteria
Daily	0.830	0.309	0.589	-9.197	Unsatisfactory	Unsatisfactory	Moderate	Very Good
Monthly	0.534	0.704	0.842	2.373	Good	Good	Very Strong	Very Good
Annual	3.087	-13.29	0.998	-5.139	Unsatisfactory	Unsatisfactory	Very Strong	Very Good

Source: Analysis Results (2025).

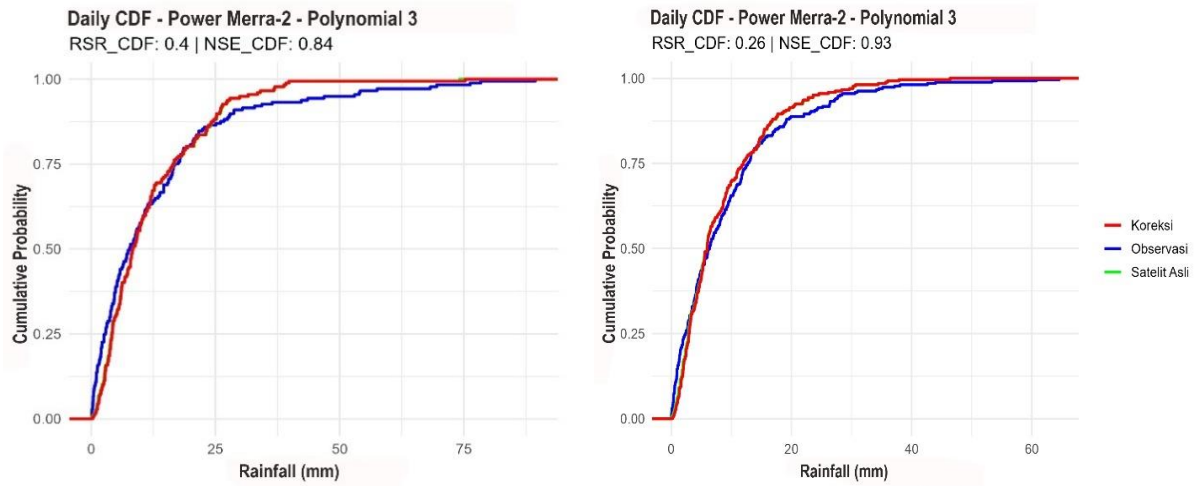

Source: Analysis Results (2025).

Figure 12. CDF Graph Results of Verification 2 and

IV. CONCLUSION

The PERSIANN-CCS satellite product has the smallest grid size and the largest number of spatial grids (14 grids), resulting in greater variability in rainfall estimates. However, when compared with rain gauge observations, noticeable discrepancies are observed between extreme rainfall and minimum rainfall values. In contrast, GSMaP and Power MERRA-2 exhibit rainfall patterns that are more consistent with rain gauge observations.Regarding rainfall classification, the calibration dataset comprises 60% normal and 40% wet years, with no dry years included, while the verification dataset does not include wet years. Based on the calibration and validation results, the Power MERRA-2 satellite product corrected using the third-order polynomial method demonstrates the best validation performance among the other five methods across daily, monthly, and annual periods.

Based on the calculation scenarios, although the calibration dataset does not include dry-year rainfall, Verification Scenario 1, which incorporates both dry and normal rainfall years, demonstrates satisfactory validation performance at the annual and monthly scales, but shows unsatisfactory performance at the daily scale. In Verification Scenario 2, which includes only normal rainfall years, validation performance at the daily scale improves to a satisfactory level. However, Verification Scenario 3, which includes only dry rainfall years, exhibits unsatisfactory performance, particularly at the daily scale. Analysis of the cumulative distribution function (CDF) indicates that rainfall values in the range of 5–25 mm are better represented in Verification Scenario 2 (normal years only) compared to Verification Scenario 3 (dry years only), in which the CDF predominantly represents rainfall values in the range of 5–15 mm.

REFERENCES

[1] Kementerian Pekerjaan Umum dan Perumahan Rakyat, *Data Hujan dan Tinggi Muka Air Sungai*, Kupang: Balai Besar Wilayah Sungai Nusa Tenggara II, 2025.

[2] Kementerian Pekerjaan Umum dan Perumahan Rakyat, *"*Progres pembangunan Bendungan Manikin capai 66%, dukung ketahanan pangan di Kupang", *Sahabat PU – Media & Informasi*, 2025.

[3] Soewarno, *Hidrologi: Aplikasi Metode Statistik untuk Analisis Data Jilid 1*, Bandung: Nova, 1995.

[4] The NASA Prediction of Worldwide Energy Resources (Power) Project, "Power Data Access Viewer", 2025, https://power.larc.nasa.gov/data-access-viewer/?

[5] Japan Science and Technology Agency (JST), ***"JAXA GSMaP Rainfall Data*** (2003–2025)," 2025, https://sharaku.eorc.jaxa.jp/GSMaP/.

[6] Center for Hydrometeorology and Remote Sensing (CHRS), "CHRS Rainfall Data (2003–2025)," 2025, https://chrsdata.eng.uci.edu/.

[7] Direktorat Jenderal Sumber Daya Air, Satuan Kerja Balai Bendungan, Petunjuk Teknis *Analisis Hidrologi dan Debit Banjir Bendungan*, 2017.

[8] D. Harisuseno, J. S. Fidari, and S. N. Aulia, "Development of isohyet map of design rainfall at various return periods in Sadar sub-watershed," ***Civilla: J. Teknik Sipil Universitas Islam Lamongan***, vol. 9, no. 2, pp. 157–170, 2024.

[9] Suni, Y. P. K., "Evaluasi hubungan data hujan satelit PERSIANN-CDR dan data hujan pengukuran DAS Liliba," *in Proc. Semin. Nas. Riset dan Teknologi Terapan (RITEKTRA)*, 2021.

[10] Krisnayanti, D. S., et al., "Evaluation of GPM IMERG product against ground station rainfall data in semi-arid region," ***Civil Engineering Journal***, vol. 10, no. 12, 2024.

[11] Krisnayanti, D. S., et al., "Evaluasi kesesuaian data Tropical Rainfall Measuring Mission (TRMM) dengan data pos hujan pada DAS Temef di Kabupaten Timor Tengah Selatan," ***Jurnal Sumber Daya Air***, vol.16, no.1, 2024.

[12] Gerland, A., "Validasi data model prediksi curah hujan satelit GPM, GSMaP, dan CHIRPS selama periode siklon tropis Seroja 2021 di Provinsi Nusa Tenggara Timur," ***GEOGRAPHIA Jurnal Pendidikan dan Penilitian Geografi***, vol. 4, no. 1, pp. 44–50, 2023.

[13] M. Okirya and A. Du Plessis, "Evaluating bias correction methods using annual maximum series rainfall data," *Hydrology*, vol. 12, no. 5, art. no. 113, 2025. https://doi.org/10.3390/hydrology12050113

[14] N. Wahi, A. Sarma, and S. K. Gorti, "Assessment of various rainfall bias correction methods including delta method," *in Proc. 2023 Int. Conf. on Modelling, Simulation, and Applied Mathematics*, 2023, pp. 114–129.

[15] D. Maraun, F. Widmann, J. Gutiérrez, S. Kotlarski, and R. Chandler, "Bias correcting climate change simulations – a critical review," *Earth System Dynamics*, vol. 8, no. 4, pp. 1041–1074, 2017.

[16] X. Li, Y. Chen, Z. Wang, and J. Li, "Statistical bias correction of precipitation forecasts based on quantile mapping," *Remote Sensing*, vol. 15, no. 7, art. no. 1743, 2023.

[17] Almira, A. H., "Koreksi bias data hujan satelit PERSIANN sebagai alternatif pos stasiun hujan dengan pendekatan quantile mapping di Sub DAS Brantas Hulu," ***Jurnal Talenta Sipil Fakultas Teknik Universitas Batanghari***, vol. 7, no. 2, pp. 595–608, 2024.

[18] Y. Song and E.-S. Chung, "Intercomparison of bias correction methods for precipitation of multiple climate models," *Geoscientific Model Development*, vol. 18, no. 4, pp. 8017–8045, 2025.

[19] D. N. Moriasi, M. W. Gitau, N. Pai, and P. Daggupati, "Hydrologic and water quality models: performance measures and evaluation criteria," *Trans. ASABE,* vol. 58, no. 6, pp. 1763–1785, 2015.

[20] A. Khalil et al., "Inhomogeneity detection in the rainfall series for the Mae Klong River Basin, Thailand," Applied Water Science, vol. 11, art. 147, 2021.

[21] B. Đurin, N. Kranjčić, S. Kanga, S. K. Singh, N. Sakač, Q. B. Pham, J. Hunt, D. Dogančić, and F. Di Nunno, "Application of Rescaled Adjusted Partial Sums (RAPS) method in hydrology – an overview," *Advances in Civil and Architectural Engineering*, vol. 13, no. 25, pp. 58–72, Dec. 2022.

[22] ***Journal of Information Systems Engineering and Management***, "Rainfall estimation methods including Thiessen Polygon for areal average rainfall calculation," ***Journal of Information Systems Engineering and Management***, vol. 10, no. 56s, 2025.

[23] Badan Meteorologi, Klimatologi, dan Geofisika, *Data Hujan Harian 2001-2020*. Stasiun Klimatologi Lasiana, 2021.

[24] Kementerian Agraria dan Tata Ruang/Badan Pertanahan Nasional, *Unduh Data DEMNAS*, 2025. Available: https://tanahair.indonesia.go.id/portal-web/unduh/demnas

[25] Badan Meteorologi, Klimatologi, dan Geofisika, *Modul pelatihan informasi cuaca maritim untuk nelayan tangkap*. Stasiun Meteorologi Maritim Tanjung Perak, 2017. Available: https://stamet-juanda.bmkg.go.id/home/data/buletin/Modul-PICM-Nelayan-Tangkap.pdf

[26] D. S. Wilks, Statistical Methods in the Atmospheric Sciences, 3rd ed. Oxford, U.K.: Academic Press, 2011.

[27] L. N. Ndoki, K. Awo, dan N. Manao, *Laporan Hasil Pengamatan di Stasiun Klimatologi Kupang*, Universitas Nusa Cendana, Kupang, Indonesia, 2022.

[28] Martha, J. W., dan Adidarma, W., Mengenal Dasar-Dasar Hidrologi. Bandung: Nova, pp.190-191, 1978.

[29] C. D. Soemarto, *Hidrologi Teknik*. Jakarta, Indonesia: Erlangga, 1987.

[30] Mukaka, M. M., "Statistics corner: A guide to appropriate use of correlation coefficient in medical research," ***Malawi Medical Journal***, 2012

[31] N. Yao, J. Ye, S. Wang, S. Yang, Y. Lu, dan X. Yang, "Bias correction of hourly satellite precipitation products using machine learning methods enhanced with high-resolution meteorological simulations," *Atmos. Res*., vol. 310, art. no. 107637, 2024, doi:10.1016/j.atmosres.2024.107637.

[32] J. Ye, Y. Lu, X. Yang, Z. He, P. Huang, dan X. Zheng, "Bias correction of hourly satellite precipitation products and their application in hydrological modeling in a hilly watershed," *Water*, vol. 16, no. 1, art. 49, 2024, doi:10.3390/w16010049.

[33] L. Wei et al., "Evaluation of seventeen satellite-, reanalysis-, and gauge-based precipitation products for drought monitoring," *Atmos. Res*., 2021.

[34] G. F. Ziarh, S. Shahid, T. Ismail, M. Asaduzzaman, dan A. Dewan, "Correcting bias of satellite rainfall data using physical empirical model," *Atmos. Res*., vol. 251, 2021, doi:10.1016/j.atmosres.2020.105430.

[35] M. Saber dan K. K. Yilmaz, "Evaluation and bias correction of satellite-based rainfall estimates for modelling flash floods," *Water*, vol. 10, no. 5, art. 657, 2018, doi:10.3390/w10050657.